Identification of gaseous oxygen and nitrogen in bubble inclusions in Bi4(GeO4)3 (BGO) crystals by means of Raman spectroscopy

Boer, R.C. de; Loosdrecht, P.H.M. van; Meekes, H.L.M.

Published in:
Journal of Crystal Growth

DOI:
10.1016/0022-0248(94)90311-5

ELSEVIER

Journal of Crystal Growth 140 (1994) 361–364

JOURNAL OF CRYSTAL GROWTH

Identification of gaseous oxygen and nitrogen in bubble inclusions in $Bi_4(GeO_4)_3$ (BGO) crystals by means of Raman spectroscopy

R.C. de Boer *, P.H.M. van Loosdrecht, H.L.M. Meekes

RIM Laboratory, Faculty of Science, University of Nijmegen, Toernooiveld, 6525 ED Nijmegen, Netherlands

(Received 1 February 1994)

Abstract

Bubble inclusions in BGO crystals have been studied by means of Raman spectroscopy. Since the crystals were grown under ambient atmospheric conditions, we focused our attention on oxygen and nitrogen. Both species are diatomic homonuclear molecules which are vibrationally and rotationally Raman active. Concerning the vibrational part of the O_2 and N_2 Raman spectra, no evidence was found for the presence of both gases. However, in the spectrum below the lowest 64 cm^{-1} energy mode of BGO three faint peaks were found which show the characteristic features of the rotational spectra of O_2 and N_2. It was found that the composition of the inclusion atmosphere was enriched by oxygen compared to the composition of the air.

1. Introduction

Bismuth germanium oxide crystal $Bi_4(GeO_4)_3$ (abbreviated to BGO) is an interesting scintillator and electro-optical material. Single crystals are grown from the melt or from hydrothermal solution. In crystals grown from the melt, often vast amounts of bubble inclusions are found [1]. Bubble inclusions are three-dimensional defects which are common in oxide single crystals [2].

The inclusions are formed by nucleation of gaseous impurities dissolved in the melt. Favourable conditions for bubble nucleation are a gas supersaturated melt and a restricted solubility of the gaseous impurities in the solid phase compared to the melt. This means that the segregation coefficient $k_{seg} = C_{solid}/C_{melt} \ll 1$ and that the actual gas concentration in the melt, C_{melt}, exceeds the saturation concentration C_{sat}. A high gas concentration near the solidification front is usually the result of diffusion-limited mass transport in combination with a high growth rate. The possible sources of dissolved gas are the dissolution of the ambient atmosphere, the presence of gaseous impurities in the starting chemicals or the dissociation of the starting chemicals into gaseous products.

Especially dissociation of the starting chemicals is understood as an important source for bubble inclusions in oxide crystals (see ref. [3], [4] or [5]). The decomposition of Bi_2O_3 in the absence of sufficient dissolved O_2 is a possibility for the presence of bubble inclusions in BGO crystals

* Corresponding author.

SSDI 0022-0248(94)00112-Y

[6,7]. In order to identify the source of gaseous impurities and to understand the chemistry, eventually involved, it is necessary to analyse the composition of bubble inclusions qualitatively as well as quantitatively.

The chemical analysis of the inclusions comprising gaseous and liquid constituents is commonly applied in geo-chemistry and paleoclimatology [8,9]. There are destructive and non-destructive methods of analysis. In the destructive type, a crystalline sample is crushed in order to open the inclusions. The contents of several inclusions are analysed by means of mass-spectroscopy or gas-chromatography. Due to the ability to accumulate sufficient material, a quantitative analysis can be carried out, which provides the average inclusion composition. The non-destructive methods are microthermometry (especially employed in geo-chemistry) and optical spectrometry. The spectroscopic techniques require that the crystalline host does not absorb or modify the radiation absorbed or emitted by the chemical species in the inclusions. Raman spectrometry fulfills this requirement since it allows the use of wavelengths which are not absorbed by the host material. For inclusion analyses, a laser Raman microprobe (LRM) apparatus can be used. This is actually a Raman spectrometer coupled to a reflection microscope. With this technique it is possible to study solitary inclusions. A major limitation is that the quantum efficiency for the Raman process is very low. Therefore the LRM spectrometer should be a highly sophisticated apparatus with low detection limits.

In the case of BGO, we are interested in oxygen and other atmospherical gases like nitrogen. Up till now it was not possible to identify the composition of bubble inclusions with mass-spectroscopy [10]. Since O_2 and N_2 are homonuclear molecules, they are vibrational and rotational Raman active. The Raman active modes of BGO show no overlap with the vibration frequencies of O_2 and N_2. Below the lowest 64 cm^{-1} Raman active lattice mode of BGO, there is no overlap with the pure rotational frequencies of O_2 and N_2. This opens the opportunity to study O_2 and N_2 inside the inclusions occurring in BGO crystals.

2. Experimental procedure

The samples examined by Raman spectroscopy are cut from BGO crystals grown from the melt by means of the Czochralski method. During the growth process, the melt and crystal are in direct contact with the ambient atmosphere, so that the atmospheric gases O_2, N_2 and CO_2 are able to dissolve in the melt. Sample slices are taken from the parts of the crystal volume with a high bubble number density (200–300 cm^{-3}). The highest bubble densities are usually found in inclusion striations which are caused by growth rate fluctuations [11]. The slices are subsequently polished on both sides before examination.

First, a microscopical inspection is carried out in order to characterize the optical transparency, the shape and the size of the inclusions. For the Raman measurement we looked for optically transparent, spherical inclusions in the order of 20 μm in diameter. Second, a slice containing inclusions which satisfy the above requirements is mounted to the microscope stage attached to the Raman spectrometer. The LRM analysis is performed with a DILOR *XY* spectrometer comprising an Ar^+ laser source ($\lambda = 514.5$ nm), a microscope and a triple monochromator in combination with a linear 1024 diode array detector. After selection of suitable intact inclusions just below the slice surface (depth < 100 μm), the microscope is switched to the Raman mode. A probe beam (power < 50 mW at $T = 295$ K) is focused inside the inclusion and the Stokes Raman spectrum is recorded in 178 subsequent accumulations, each lasting 10 s integration time. After collection of sufficient data to identify gaseous constituents, the data acquisition is terminated. Then, the microscope mode is installed and the sample slice is translated to a crystal volume free from bubble inclusions, to be sure that the sensing volume contains no gaseous species. Then a reference spectrum is recorded from this part of the crystal volume under the same conditions as described above. Subsequently, the spectra are verified for the presence of vibrational and rotational lines of O_2 and N_2. Since only the matter in the sensing volume contributes to the measured signal, no special pre-

cautions need be taken in order to avoid contamination by O_2 and N_2 present in the atmosphere.

3. Results

The Raman spectra are checked for the presence of Raman active molecular vibrations of O_2 ($\nu = 1580$ cm^{-1}) and N_2 ($\nu = 2331$ cm^{-1}) and rotations of O_2 ($B = 1.446$ cm^{-1}) and N_2 ($B = 1.9987$ cm^{-1}). BGO has no Raman active modes in the spectral regions of interest.

Concerning the characteristic molecular vibrations, no evidence is found for the presence of O_2 and N_2. A representative Raman spectrum (unpolarized) of BGO is shown in Fig. 1. The spectral window for rotational transitions is marked by the dashed frame in the low energy part of the spectrum between the Rayleigh peak at 0 cm^{-1} and the lowest energy active Raman mode of BGO 64 cm^{-1} [12]. An enlarged view of this spectral window is shown in Fig. 2, representing the spectrum of the inclusion constituents (A), a reference spectrum of pure BGO (B) and the spectrum of air (C). The three spectra are shifted in vertical position to avoid overlap. The difference in scattering cross-section between the inclusion constituents and the BGO host as revealed by Fig. 1 is mainly caused by a large difference in mass density, because the Raman scattering intensity is proportional to the number of particles in the sensing volume. However, one should not neglect the differences in intrinsic quantum efficiency, although they are not known.

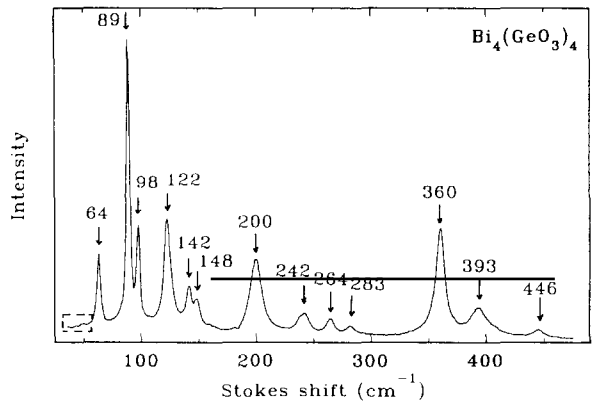

Fig. 1. Unpolarized Raman spectrum of single-crystalline $Bi_4(GeO_4)_3$ at $T = 300$ K. The spectrum is recorded using 514.5 nm excitation with a laser power of 100 mW. The dashed frame contains the spectrum of the inclusion contents.

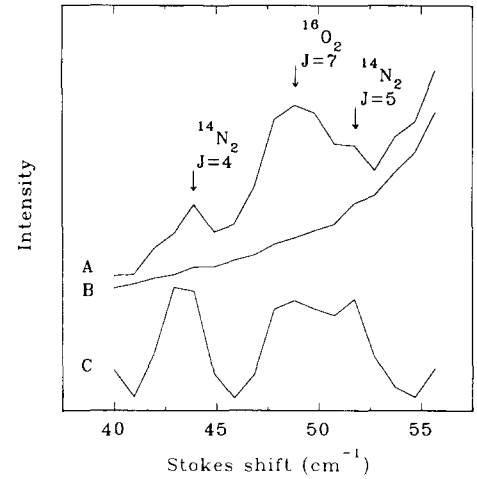

Fig. 2. Detailed Raman spectrum in the range between 40 and 60 cm^{-1}: (A) the spectrum of the inclusion contents, (B) the background spectrum of $Bi_4(GeO_4)_3$ and (C) the reference air spectrum. The peaks at 43.9 and 51 cm^{-1} belong to N_2 and the peak at 48.9 cm^{-1} belongs to O_2. The A and B spectra are vertically shifted with respect to the C spectrum to avoid overlap.

4. Discussion

The inclusion spectrum (A) reveals three distinct peaks at 43.9, 48.9 and 51.8 cm^{-1}, which are superimposed on the left flank of the 64 cm^{-1} BGO peak. These peaks can be interpreted as pure rotational transitions of $^{14}N_2$ and $^{16}O_2$. Rotational Raman scattering obeys the selection rule $\Delta J = \pm 2$. The Stokes line with Raman frequency ν corresponds to the transition for the initial rotation level J_0 to the final rotation level $J_0 + 2$:

$$\nu = \nu_0 - 2B(2J_0 + 3), \quad (1)$$

where ν_0 represents the Rayleigh frequency and B the rotational constant, all in cm^{-1}. The distance between two successive spectral lines, with the initial levels J_0 and $J_0 + 1$, is equal to $4B$. The rotational constant of $^{14}N_2$ is 1.989 cm^{-1}

and the peaks at 43.9 and 51.8 cm^{-1} correspond to the states $J_0 = 4$ and $J_0 = 5$, respectively. The intensity difference between the $J_0 = 4$ peak and the $J_0 = 5$ peak is due to the nuclear spin, and according to Brodersen [14] the intensities of even rotation lines are twice as strong as the intensity of odd rotation lines. The rotational constant of $^{16}O_2$ equals 1.438 cm^{-1} and only odd numbered rotational levels are allowed [13]. Then a simple calculation using Eq. (1) predicts one rotation line at 48.9 cm^{-1} for $J_0 = 7$ in spectral range between 40 and 55 cm^{-1}.

The lack of vibration lines of these species is not in conflict with the presence of rotation lines, since pure rotation transitions usually have a larger scattering cross-section than vibration–rotation transitions [14]. The limited part of the Raman spectrum (40–64 cm^{-1}) implies that the bubble inclusions comprise at least gaseous oxygen and nitrogen. The fact that other gaseous substances are not identified does not exclude there presence. The presence of nitrogen proves that dissolution of gases from the ambient atmosphere into the melt took place. An important difference between the inclusion spectrum (A) and the air reference spectrum (C) is that the intensity ratio $I(O_2)/I(N_2)$ in the inclusion spectrum is larger than the intensity ratio in the air spectrum. Since the intensity is a measure for the concentration, it indicates that the fraction O_2 in the inclusion gas is larger than the fraction O_2 in the air. The fact that the gas composition inside the inclusion is enriched with O_2 can indicate a difference between the segregation of O_2 and N_2 or it indicates melt decomposition. However, we are not able to verify which effect is relevant in the present experiment.

5. Conclusion

By means of LRM, oxygen and nitrogen are identified as gaseous constituents in bubble inclusions occurring in BGO crystals. This sophisticated technique opens the possibility to conduct non-destructive experiments concerning the role of chemistry in bubble inclusion formation in BGO and other oxide crystals. The presence of nitrogen proves that dissolution of gases from the ambient atmosphere is a relevant source for the bubble formation. The fraction O_2 in the inclusion gas is larger than the fraction O_2 in air. This oxygen enrichment is possibly caused by segregation or by melt decomposition. However, we were not able to find out whether melt decomposition is responsible for the presence of oxygen in the bubble inclusions.

Acknowledgments

P. van Loosdrecht acknowledges the financial support of the Dutch Foundation for Fundamental Research of Matter and R. de Boer wishes to thank for financial support by Quartz & Silice.

References

[1] A. Horowitz and G Kramer, J. Crystal Growth 79 (1986) 296.
[2] B. Cockayne, in: Current Topics in Materials Science. Vol. 2, Ed. E. Kaldis (North-Holland, Amsterdam, 1977) p. 503.
[3] C.D. Brandle, D.C. Miller and J.W. Nielsen, J. Crystal Growth 12 (1972) 195.
[4] K.S. Bagdasarov and G. Arzumanyan, Kristallografiya 33 (1988) 1040.
[5] S. Uda and W.A. Tiller, J. Crystal Growth 121 (1991) 155.
[6] P.C. Chaubal and M. Nagamori, Met. Trans. B, 13B (1982) 339.
[7] E. Beck and S. Kemmler-Sack, J. Less-Common Metals 135 (1987) 257.
[8] A.M. Van der Kerkhof and S.N. Olsen, Geochim. Cosmochim. Acta 54 (1990) 895.
[9] J.L. Pasteris, B. Wopenka and J.C. Seitz, Geochim. Cosmochim. Acta 52 (1988) 979.
[10] P. Schotanus, private communication.
[11] F. Smet and W.J.P. van Enckevort, J. Crystal Growth 88 (1989) 169.
[12] M. Couzi, J.R. Vignalou and G. Boulon, Solid State Commun. 20 (1976) 461.
[13] G. Herzberg, in: Molecular Spectra and Molecular Structure, 1, Spectra of Diatomic Molecules, 2nd ed. (Van Nostrand, New York, 1950).
[14] S. Brodersen, in: Raman Spectroscopy of Gases and Liquids, Ed. A. Weber (Springer, Berlin, 1979) p. 7;
A. Weber, in: Raman Spectroscopy of Gases and Liquids, Ed. A. Weber (Springer, Berlin, 1979) p. 70.